

Monolithic Whispering-Gallery Mode Resonators With Vertically Coupled Integrated Bus Waveguides

Mher Ghulinyan, Romain Guider, Georg Pucker, and Lorenzo Pavesi

Abstract—We report on the realization of a silicon-based microresonator/waveguide coupled system, fully integrated on a silicon chip. The device uses a vertical coupling scheme of the resonator and a buried strip waveguide. We demonstrate that its high optical quality follows from the accurate planarization of the waveguide topography, which is achieved by multiple depositions and reflows of a borophosphosilicate glass over strip waveguides. More importantly, we demonstrate wafer-scale mass fabrication of freestanding planar resonators suspended in air and coupled to integrated bus waveguides, as well as controlled selective excitation of different mode families of the resonator. This opens the door for the realization of stable all-integrated complex resonator systems for optomechanical and metrological applications, with the potential to substitute today's intensive use of complicated fiber-taper coupling schemes.

Index Terms—Monolithic integration, optical resonator, vertical coupling.

I. INTRODUCTION

ONE of the most important requirements for planar Whispering-gallery mode (WGM) resonators made of relatively low-index materials, such as silicon dioxide or silicon nitride, is a high refractive index contrast between the cavity and the surrounding media. For this reason, a quasi-freestanding resonator embedded in air is the preferred solution [1]. In practice, this is achieved by underetching the resonator base to form a small diameter pedestal. Most of current cutting-edge experiments with this kind of optically passive and freestanding resonators regularly uses tapered fibers to probe the system [2]–[4]. In this scheme, a tapered fiber is laterally approached to the cavity to a distance that allows an evanescent field coupling. Positioning the tapered fiber requires the use of piezoelectric controllers to provide nanometric coupling gap. This, however, results in unstable experimental conditions. In view of recent advances in the field of cavity optomechanics [2], [5], [6], the lack of a freestanding WGM cavity system monolithically integrated with an input/output waveguide reduces the chances for the applications of these devices [7].

Manuscript received April 28, 2011; accepted May 14, 2011. Date of publication May 23, 2011; date of current version July 27, 2011. This work has been supported by NAOIMI-FUPAT.

M. Ghulinyan and G. Pucker are with the Advanced Photonics and Photovoltaics Group, Bruno Kessler Foundation, Trento 38123, Italy (e-mail: ghulinyan@fbk.eu).

R. Guider was with the Nanoscience Laboratory, Department of Physics, University of Trento, Trento 38123, Italy. He is now with Johannes Kepler Universität, 4040 Linz, Austria.

L. Pavesi is with the Nanoscience Laboratory, Department of Physics, University of Trento, Trento 38123, Italy.

Color versions of one or more of the figures in this letter are available online at <http://ieeexplore.ieee.org>.

Digital Object Identifier 10.1109/LPT.2011.2157487

In planar lightwave circuits, the *vertical* coupling of a WGM resonator to a bus waveguide (the resonator and the bus waveguide lay on different planes) has several advantages with respect to the *lateral* coupling (the resonator and the bus waveguide lay on the same plane). In fact, vertical coupling:

- (i) avoids the use of ultrahigh resolution lithography, such as deep-UV or electron beam lithography to control the gap width at the nanometer level;
- (ii) permits to use different materials and thicknesses for the resonator and the waveguide;
- (iii) allows the selective exposure of the resonator or the bus waveguide to the ambient for sensing applications.

These advantages are counterbalanced by delicate fabrication processes. The most delicate process step is the planarization of the strip waveguide cladding which precedes the microdisk fabrication. Different solutions to solve this issue partially have been reported in the literature. For example, in [8] channel waveguides have been buried in SiO₂ by using a chrome liftoff technique, while in [9] a two-step InP epitaxial regrowth was used to planarize InGaAsP waveguides. In [10], [11] a simultaneous deposition/removal procedure of a deuterium rich oxynitride (SiO_xN_y:D) cladding was used. CMOS-compatible heterogenous III–V-on-SOI (Silicon on Insulator) technology uses molecular or adhesive die-to-wafer bonding to couple vertically III–V microring lasers to silicon [12]–[14]. As an adhesive layer, a polymer is used, which undergoes a pressure-assisted curing and, therefore, may result in a barely controlled coupling gap. Wafer bonding technique has been also used for the realization of an all-III–V electrically driven resonator/waveguide coupled system [15].

Here we report on the realization and optical testing of a silicon-based vertically coupled resonator system using standard silicon microfabrication technology. In particular, we used multiple depositions and reflows of a borophosphosilicate glass (BPSG) in order to planarize the cladding over the strip waveguides and simultaneously define the vertical coupling gap. An accurate control of both layer thicknesses and degree of planarization (DOP) can be achieved¹. Furthermore, we have developed a technology to realize freestanding WGM resonators suspended over the bus waveguides, thus, demonstrating an effective air coupling in an integrated system. Waveguide transmission measurements revealed quality factors of $\sim 20,000$ from very first devices.

II. RESULTS AND DISCUSSION

The device fabrication process starts with a plasma enhanced chemical vapor deposition (PECVD) of a 2 μm -thick SiO₂

¹The degree of planarization (DOP) is defined as the relative reduction in height of any step-like feature present on an otherwise flat surface. In our case this feature is caused by the buried waveguide.

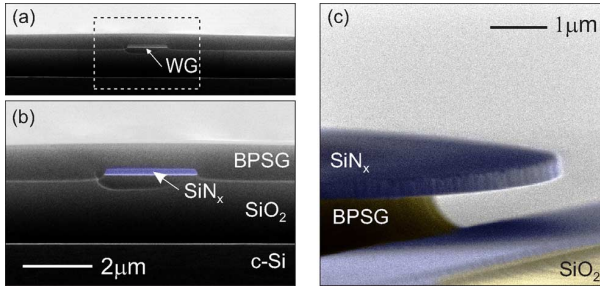


Fig. 1. SEM images (false-colored) of the device. (a) The cross-sectional image shows a quasi-full planarization of the strip waveguide. (b) A close-up of the waveguide facet. (c) A tilted angle view of the vertical coupling zone between the waveguide and air suspended microdisk resonator.

cladding layer on a crystalline Si wafer. Then, a 260 nm PECVD SiN_x layer is deposited on top of the cladding, patterned lithographically and successively dry-etched to form strip waveguides. The dry etching procedure, accounting for the cladding overetch, results in a step-height of 350 nm at the waveguide edges. Without planarization, such a topography will be transferred to the coupling silica spacer and, finally, to the resonator layer, resulting in an extremely lossy device.

Therefore, we performed a surface planarization step using a BPSG layer, which offers excellent step-coverage and reflow characteristics [16], [17]. We first deposited a 700 nm-thick BPSG layer by low pressure chemical vapor deposition and reflowed it at 1000°C for 1 hour in an N_2 atmosphere. This resulted in a DOP of $55\% \pm 2\%$ around $2.5 \mu\text{m}$ -wide waveguides. Successively, we deposited other 700 nm's of BPSG and reflowed it. The multiple deposition/reflow procedure improves continuously the surface planarity, since each new deposition starts from a smoother topography. In fact, after only two steps, a DOP of $88\% \pm 2\%$ was extracted from scanning electron microscopy (SEM) images (Fig. 1(a), (b)), which is comparable to the state-of-the-art of 90%, achieved through polymer-planarization [12], [13]. Then, the BPSG thickness was reduced by a wet etch in order to define the vertical coupling gap. The final gap thickness within a precision of 5 nm ($\sim 0.6\%$ of a typical vertical gap of 800 nm) is controlled using an optical interferometer. Finally, a 350 nm-thick PECVD SiN_x layer was deposited, and WGM resonators were defined through standard photolithographic and dry etching steps. As a result, monolithic microresonators vertically coupled to buried waveguides were realized (Fig. 2(a)–(c)).

The devices were characterized by measuring the bus waveguide transmission with a near-infrared tunable laser butt-coupled to the bus waveguide. The signal polarization was controlled at the waveguide input and analyzed at its output. A beam splitter was used to simultaneously monitor the transmitted mode profile with an infrared CCD camera and to measure the transmitted signal intensity with a photodiode.

Here we report on the results obtained from $50 \mu\text{m}$ -diameter microdisk resonators. To demonstrate the potential of the described technological approach we studied three WGM devices with the same coupling gap of 850 nm but different lateral alignments between the microdisk and the bus waveguide (Fig. 2(a)–(c)). The alignment is described by the parameter Δ which measures the position of the disk edge relative to the waveguide axis. Fig. 2(d) shows the transmission spectra

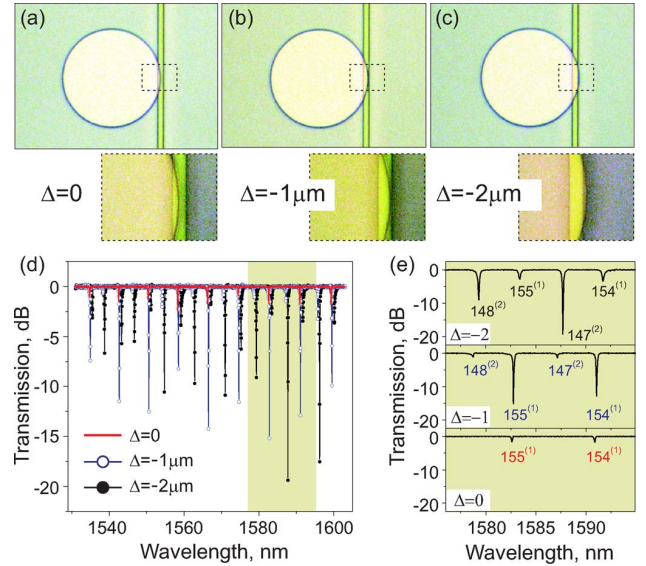


Fig. 2. Top-view optical images of WGM microdisks vertically coupled to bus waveguides. The parameter Δ is the lateral distance between the microdisk edge and the waveguide axis: (a) $\Delta = 0$, (b) $-1 \mu\text{m}$, and (c) $-2 \mu\text{m}$. (d) Normalized transmission spectra over a wide wavelength range. (e) Zoom of the spectra around $\lambda \approx 1585 \text{ nm}$. The different resonances are labeled with their corresponding radial and azimuthal mode numbers.

from these devices². A series of transmission dips (cavity resonances) due to the coupling of the signal into the microdisk is observed. The homogenous distribution of cavity resonances throughout the whole spectrum with a mean quality factor of $\bar{Q} \approx 20,000$ confirms the good optical quality of the microdisks, i.e., of the planarization process. Moreover, statistical analysis of transmission performed over many $50 \mu\text{m}$ resonators (same Δ) from different wafers resulted in a less than 1 nm spectral variation of WGM peak positions. Finite element analysis suggests that this corresponds to a diameter variation of less than 40 nm, which implies an excellent wafer scale mass fabrication of WGM resonators with a size deviation of 0.08% only.

In Fig. 2(e) we show the high-resolution transmission spectra around $\lambda = 1585 \text{ nm}$ for different Δ values. Different spectra are observed even though the same coupling gap is used. Firstly, we performed finite element simulations in order to identify the observed modal structure of the resonator (radial families, p , and azimuthal mode numbers M , labeled as $M^{(p)}$ hereafter). From the bottom panel of Fig. 2(e) we see that for $\Delta = 0$, only the first radial mode family, with a free spectral range of FSR $\approx 8 \text{ nm}$, is excited ($154^{(1)}$, $155^{(1)}$). For $\Delta = -1 \mu\text{m}$ (central panel of Fig. 2(e)), this family is more efficiently excited while modes with $p = 2$, ($147^{(2)}$, $148^{(2)}$), appear in the spectrum. A larger overlap between the bus waveguide and the microdisk inverts the relative intensities of the mode families (top panel, Fig. 2(e)). For this Δ value, $M^{(2)}$ modes are spatially aligned to the waveguide. This result shows another advantage of the vertical coupling scheme; it allows for a selective excitation of different mode families, which is impossible to achieve with lateral coupling.

More importantly, the proposed approach enables the realization of freestanding WGM resonators suspended in air over

²The raw spectra were normalized to the transmission spectra of a bare waveguide on the same chip.

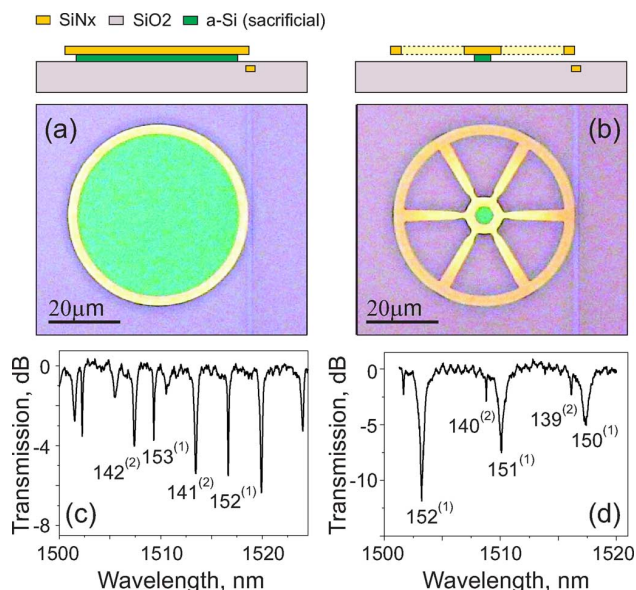


Fig. 3. Free-standing WGM resonators with monolithically integrated bus waveguides. Optical micrographs of (a) a raised microdisk resonator and (b) a spiderweb ring resonator with corresponding cross-sectional sketches (top panels). The transmission spectra, plotted in (c) and (d), show the presence of WGM resonances with quality factors of the order of $(1 \div 2.5) \times 10^4$ depending on the coupling strength of various modes $M^{(p)}$.

the bus waveguides. This, for example, can be achieved by a partial removal of BPSG under the resonator using a selective wet etch as shown in Fig. 1(c). In specific cases, when a deep underetch is required, one may use a sacrificial layer between the resonator and the planarized BPSG in order to prevent the waveguide from damaging (see the cross-sectional sketches in Fig. 3). As described in the following, the sacrificial layer can be removed isotropically through either a selective chemical wet or dry etching, leaving the cladding BPSG layer, and, therefore, also the waveguide unaffected.

In Fig. 3(a) and (b) top-view optical images of a freestanding WGM microdisk and a spiderweb ring resonator air-coupled to the bus waveguides are shown. In this case, after the planarization, the BPSG layer was reduced to approximately 300 nm and covered by a 250 nm-thick amorphous silicon (a-Si) layer. After the deposition and definition of SiN_x microresonators, the a-Si layer was selectively removed by using an isotropic dry Si deep reactive ion etch. The underlying BPSG layer remained unaffected. Thus, WGM resonators suspended in air over the cladded bus waveguides were successfully realized. We note, that a similar free-standing resonator system consisting of resonators vertically coupled to the waveguides has been reported in past using a wafer-to-wafer bonding process [18]. The device was realized on a SOI platform and was MEMS-actuated to provide a tunable vertical coupling.

The transmission spectra of the suspended microresonators are plotted in Fig. 3(c) and (d). The resonant nature of the optical devices is clearly seen, and the various $M^{(p)}$ modes can be identified. We note that the vertical coupling gaps for these first devices were not optimized. While the microdisk spectrum is characterized by narrow resonances, the spiderweb shows rather broad first radial family modes. On one side, the spiderweb resonator possesses a lower effective refractive index and therefore a weaker mode confinement with respect to the microdisk.

On the other side, the residual film stress after the underetch bends the spiderweb towards the waveguide pushing it into a stronger coupling regime. Both effects, therefore, result in lower quality factors for the spiderweb resonator, which can be improved through a careful optimization of the design and processing.

In conclusion, we have demonstrated wafer-scale integration of a monolithic planar microresonator/waveguide vertically coupled system on a silicon chip. An easily accessible technological approach has been implemented for the realization of silicon-based freestanding WGM resonators suspended over the integrated bus waveguides with Q 's of 20,000 from very first devices. The described solutions can be exploited not only for the developments of compact Si-based lightwave circuits, but more importantly, can bring to the industrial market all-integrated optomechanics with WGM resonators [5], [6].

ACKNOWLEDGMENT

The authors wish to thank A. Pitanti and P. Bettotti for stimulating discussions.

REFERENCES

- [1] *Practical Applications of Microresonators in Optics and Photonics*, A. B. Matsko, Ed., Boca Raton, FL: CRC Press, 2009.
- [2] T. J. Kippenberg and K. J. Vahala, "Cavity optomechanics: Back-action at the mesoscale," *Science*, vol. 321, no. 5893, pp. 1172–1176, 2008.
- [3] P. Del'Haye, A. Schliesser, O. Arcizet, T. Wilken, R. Holzwarth, and T. J. Kippenberg, "Optical frequency comb generation from a monolithic microresonator," *Nature*, vol. 450, no. 7173, pp. 1214–1217, 2007.
- [4] I. S. Grudin, H. Lee, O. Painter, and K. J. Vahala, "Phonon laser action in a tunable two-level system," *Phys. Rev. Lett.*, vol. 104, no. 8, pp. 083901(1)–(4), 2010.
- [5] P. T. Rakich, M. A. Popović, M. Soljačić, and E. O. Ippen, "Trapping, corralling and spectral bonding of optical resonances through optically induced potentials," *Nature Photon.*, vol. 1, no. 11, pp. 658–665, 2007.
- [6] G. S. Wiederhecker, L. Chen, A. Gondarenko, and M. Lipson, "Controlling photonic structures using optical forces," *Nature*, vol. 462, no. 7273, pp. 633–636, 2009.
- [7] B. Redding, E. Marchena, T. Creazzo, S. Shi, and D. W. Prather, "Comparison of raised-microdisk whispering-gallery-mode characterization techniques," *Opt. Lett.*, vol. 35, no. 7, pp. 998–1000, 2010.
- [8] B. E. Little *et al.*, "Vertically coupled glass microring resonator channel dropping filters," *IEEE Photon. Technol. Lett.*, vol. 11, no. 2, pp. 215–217, Feb. 1999.
- [9] S. J. Choi *et al.*, "Microring resonators vertically coupled to buried heterostructure bus waveguides," *IEEE Photon. Technol. Lett.*, vol. 16, no. 3, pp. 828–830, Mar. 2004.
- [10] M. Ferrera *et al.*, "Low-power continuous-wave nonlinear optics in doped silica glass integrated waveguide structures," *Nature Photon.*, vol. 2, no. 12, pp. 737–740, 2008.
- [11] L. Razzari *et al.*, "CMOS-compatible integrated optical hyper-parametric oscillator," *Nature Photon.*, vol. 4, no. 1, pp. 41–45, 2009.
- [12] G. Roelkens, D. Van Thourhout, R. Baets, R. Nötzel, and M. Smit, "Laser emission and photodetection in an InP/InGaAsP layer integrated on and coupled to a silicon-on-insulator waveguide circuit," *Opt. Express*, vol. 14, no. 18, pp. 8154–8159, 2006.
- [13] L. Liu *et al.*, "An ultra-small, low-power, all-optical flip-flop memory on a silicon chip," *Nature Photon.*, vol. 4, no. 3, pp. 182–187, 2010.
- [14] P. Viktorovitch *et al.*, "3D harnessing of light with 2.5D photonic crystals," *Las. Photon. Rev.*, vol. 4, no. 3, pp. 401–413, 2010.
- [15] A. Benneker, K. A. Williams, R. V. Pentyl, I. H. White, M. Hamacher, and H. Heidrich, "Directly-modulated multi-wavelength-multiplexed integrated microring laser array," *IEEE Photon. Technol. Lett.*, vol. 20, no. 16, pp. 1411–1413, Aug. 15, 2008.
- [16] M. Susa *et al.*, "Borophosphosilicate glass flow for solid-state imager application," *J. Appl. Phys.*, vol. 58, no. 10, pp. 3880–3883, 1985.
- [17] H. Rong *et al.*, "Low-threshold continuous-wave Raman silicon laser," *Nature Photon.*, vol. 1, no. 4, pp. 232–237, 2007.
- [18] M.-C. M. Lee and M. C. Wu, "Tunable coupling regimes of silicon microdisk resonators using MEMS actuators," *Opt. Express*, vol. 14, no. 11, pp. 4703–4712, 2006.